

**ISE**

Industrial and  
Systems Engineering

# Truss topology design optimization with guaranteed kinematic stability

MOHAMMAD SHAHABSAFA, RAMIN FAKHIMI, WEIMING LEI , TAMÁS  
TERLAKY, AND LUIS ZULUAGA

Dept. of Industrial and Systems Engineering  
Lehigh University, Bethlehem, PA, USA

SICHENG HE, JOHN T. HWANG, AND JOAQUIM R. R. A. MARTINS

Dept. of Aerospace Engineering  
University of Michigan, Ann Arbor, MI, USA

ISE Technical Report 17T-015



**LEHIGH**  
UNIVERSITY.

# Truss topology design optimization with guaranteed kinematic stability

MOHAMMAD SHAHABSAFA<sup>1</sup>, RAMIN FAKHIMI<sup>1</sup>, WEIMING LEI<sup>1</sup>, TAMÁS TERLAKY<sup>1</sup>, LUIS ZULUAGA<sup>1</sup>, SICHENG HE<sup>2</sup>, JOHN T. HWANG<sup>2</sup>, AND JOAQUIM R. R. A. MARTINS<sup>2</sup>

<sup>1</sup> Dept. of Industrial and Systems Engineering, Lehigh University, Bethlehem, PA, USA ,  
<sup>2</sup> Dept. of Aerospace Engineering, University of Michigan, Ann Arbor, MI, USA

August 12, 2019

## Abstract

Kinematic stability of the truss topology design and sizing optimization (TTDSO) problems is a crucial aspect which is often overlooked in the mathematical optimization models. In this paper, we propose a novel mathematical optimization model for the discrete TTDSO problem with Euler buckling constraints. Random perturbations of external forces are used to obtain kinematically stable structures. We prove that by considering the perturbed external forces, the resulting structure is kinematically stable with probability one. Furthermore, we show that necessary conditions for kinematic stability can be used to speed up the solution of discrete TTDSO problem. While mixed integer linear optimization (MILO) solvers for existing models are not able to even find a feasible solution for Michell trusses with more than 182 bars in a reasonable amount of time, our model provides high-quality solutions for those problems in the same time window.

## 1 Introduction

The truss design problem is an important problem in the field of structural design optimization (Haftka and Gürdal, 2012). In the past century, various formulations and solution methodologies for truss design problems are developed (Arora and Wang, 2005; Rozvany, 2009; Stolpe, 2016). Dorn et al. (1964) considered a ground structure framework for the truss design problem and used numerical optimization to solve the problem. In a ground structure framework, the set of potential bars of a truss structure is given and the optimal bar cross-sectional areas of the bars of the structure are to be determined.

Two objectives are commonly used in truss design problems.

Namely, a wide range of mathematical models for truss design problems consider the structure's compliance minimization as the objective (Ben-Tal and Bendsøe, 1993; Bendsøe et al., 1994; Stolpe, 2007). For this problem, several second order cone optimization and semidefinite optimization models have been suggested to address the non-linearity associated with the compliance objective (Kanno, 2016; Kanno and Fujita, 2018; Ben-Tal and Bendsøe, 1993; Kanno, 2018). Another frequently used objective in truss design problems is weight minimization (Stolpe and Svanberg, 2004; Stolpe, 2004; Van Mellaert et al., 2015; Shahabsafa et al., 2018). Minimizing the structure weight or fuel burn rate, which is closely correlated with weight, are commonly considered in aerospace engineering design problems (Brooks et al., 2018; Jasa et al., 2018; Chauhan and Martins, 2018; Kennedy, 2016; Aage et al., 2017).

We focus on mixed integer linear optimization (MILO) modeling approaches which in theory leads to global optimal solution of the TTDSO problem. Due to rapid improvement of MILO solvers, we can solve

large-scale problems to optimality in a reasonable time. There are two types of truss design problems: continuous and discrete design problems. In continuous problems, all the design variables are continuous, while discrete problems involve discrete design variables. Discrete problems have three major categories: truss topology design (TTD), truss sizing optimization (TSO), and truss topology design and sizing optimization (TTDSO). [Stolpe \(2007\)](#) suggested a MILO model for compliance minimization of a TTD problem. In TSO, the topology is given and the bar cross sectional areas of the optimal bars are to be determined. [Van Mel-laert et al. \(2015\)](#) proposed a MILO model for TSO problems considering resistance and joint geometry constraints. [Shahabsafa et al. \(2018\)](#) presented several MILO models for TSO problems considering Hooke’s law, yield stress and Euler buckling constraints. In TTDSO, however, the topology and sizing of a truss are simultaneously considered. [Stolpe \(2015\)](#) considered a mixed-integer nonlinear optimization model for the TTDSO problem in which the structure maximum compliance is considered as a constraint of the model. [Stolpe \(2016\)](#) presented a comprehensive survey of discrete truss design problems.

It is assumed in TSO problems that the given ground structure is kinematically stable, while kinematic stability of the solution in TTD and TTDSO needs to be enforced. Enforcing stability in a truss structure can make the problem significantly harder to solve and thus, it is often overlooked when tackling truss design problems. [Faustino et al. \(2006\)](#) proposed a MILO model for the TTDSO problem. They considered structure kinematic stability by using Grubler’s criterion ([Ghosh and Mallik, 2002](#)), which is a necessary but not sufficient condition for having a stable structure. [Faustino et al. \(2006\)](#), additionally, proposed a perturbation of the external forces to obtain kinematically stable structures, and without formal statement, they argued intuitively that the perturbation should result in a stable structure.

However, they did not rigorously prove that the perturbation guarantees kinematic stability of the structure. [Kanno and Guo \(2010\)](#) considered an iterative external force perturbation method to obtain a kinematically stable structure for the TTDSO problem with discrete cross-sectional areas. However, their method does not guarantee kinematic stability of the structure. [Mela \(2014\)](#) developed a MILO model for minimum weight discrete TTDSO problems considering Euler buckling and displacement constraints. [Mela \(2014\)](#) also considered the kinematic stability of the structure and the issue of overlapping bars in TTDSO problems. To enforce kinematic stability of the structures, [Mela \(2014\)](#) used the external force perturbation approach which was originally proposed by [Faustino et al. \(2006\)](#). [Mela \(2014\)](#) observed that the perturbation provided stable structures for all the cases considered, but did not prove that the approach always provides a stable structure.

Guaranteed stability of the structure is a fundamentally important problem and has remained an open question in the mathematical optimization modeling framework. In this paper, we focus on the minimum-weight discrete truss topology design and sizing optimization (TTDSO) problem. We propose a novel mixed integer linear optimization (MILO) model for discrete TTDSO problems. Our models consider force balance equations, Hooke’s law, yield stress, Euler buckling constraints, and bounds on the nodal displacements. We also propose a modeling approach that ensures the kinematic stability of the structure. Furthermore, we show that the necessary conditions for kinematic stability can be used to speed-up the solution time of TTDSO problem.

The paper is structured as follows. In [Section 2](#) we overview the TTDSO problem. In [Section 3](#), we propose a novel mathematical model for the discrete TTDSO problem, and in [Section 4](#), we propose a method to enforce the kinematic stability of the structure, and prove that, with probability one, the optimal structure is kinematically stable. In [Section 5](#), we demonstrate that the proposed mathematical model can be solved significantly faster than other proposed discrete TTDSO models. Finally, our conclusions are presented in [Section 6](#).

## 2 Problem description

A truss design problem is concerned with the optimal selection of the geometry, topology, and sizing of a truss structure ([Haftka and Gürdal, 2012](#)). In this article, we focus on topology and sizing optimization of a truss. Consider a truss structure in a  $d$ -dimensional space ( $d = 2, 3$ ). Let  $m$  and  $n$  denote the number of the bars and the degrees of freedom of the ground structure, respectively. For ease of presentation, we

assume that each node of the ground structure is either fixed in all directions or pinned. Let  $\mathcal{I} = \{1, \dots, m\}$  be the index set of the bars of the ground structure and let  $\mathcal{J}$  denote the index set of the pinned nodes of the ground structure. Vector  $x \in \mathbb{R}_+^m$  denotes the cross-sectional areas of the bars, where  $\mathbb{R}_+^m$  is the set of  $m$ -dimensional non-negative vectors. A truss structure is specified when the bars and their cross-sectional areas are determined. As a result, the cross-sectional areas are the main design variables of the problem.

The force balance equations on the nodes of the truss are defined as

$$Rq = f, \quad (1)$$

where  $R \in \mathbb{R}^{n \times m}$  is the topology matrix of the truss,  $q \in \mathbb{R}^m$  is the vector of the internal forces acting on the bars, and  $f \in \mathbb{R}^n$  is the vector of the external forces exerted on the nodes. Stress on bar  $i$ , for  $i \in \mathcal{I}$ , is defined as

$$\sigma_i = \begin{cases} \frac{q_i}{x_i}, & \text{if } x_i > 0, \\ 0, & \text{otherwise.} \end{cases} \quad (2)$$

The nodal displacements and the elongation of the bars are denoted by  $u \in \mathbb{R}^n$  and  $\Delta l \in \mathbb{R}^m$ . The relationship between the nodal displacement and the elongation of the bars is as follows:

$$\Delta l = R^T u. \quad (3)$$

We define  $\lambda_i = E_i/l_i$ , for  $i \in \mathcal{I}$ , where  $E_i$  and  $l_i$  are the Young's modulus and the length of bar  $i \in \mathcal{I}$ . We consider Hooke's law, which is enforced by considering constraints (1), (2), and (3) along with the following set of constraints (Zienkiewicz and Taylor, 2005):

$$\sigma_i = \lambda_i \Delta l_i, \quad i \in \mathcal{I}. \quad (4)$$

From equations (1), (2), (3), and (4), it follows that

$$K(x)u = f,$$

where  $K(x) = \sum_{i=1}^m \lambda_i x_i r_i r_i^T$  is the stiffness matrix of the structure, and  $r_i$ , for  $i \in \mathcal{I}$ , is the  $i$ -th column of the topology matrix  $R$ .

Let  $\sigma^{\min} \in \mathbb{R}^m$  and  $\sigma^{\max} \in \mathbb{R}^m$  be the lower and upper bounds on the stress of the bars, where  $\sigma^{\min} < 0 < \sigma^{\max}$ . The stress on bars should satisfy the following constraints

$$\sigma^{\min} \leq \sigma \leq \sigma^{\max}.$$

We assume that bars' cross-sections are circular. Thus, by letting  $\gamma_i = \pi E_i / 4l_i^2$  for all  $i \in \mathcal{I}$ , the Euler buckling constraints are written as

$$\sigma_i + \gamma_i x_i \geq 0, \quad i \in \mathcal{I}, \quad x_i \neq 0.$$

For a discussion on the value of  $\gamma_i$ ,  $i \in \mathcal{I}$ , for more general cross-sectional areas of bars see our previous work (Shahabsafa et al., 2018). Let  $\mathcal{L}$  denote the index set of the coordinates of the pinned nodes of the ground structure, noting that  $|\mathcal{L}| = |\mathcal{J}|d = n$ , where  $d$  is the space dimension. The nodal displacement bound constraints are written as

$$u_\ell^{\min} \leq u_\ell \leq u_\ell^{\max}, \quad \ell \in \mathcal{L}. \quad (5)$$

### 3 Mathematical optimization model

In this section, we present mathematical optimization models for the discrete TTDSO problem, where bars takes zero or discrete valued cross-sectional areas. In other words, in the TTDSO, we allows the bars to

vanish in the final structure. These models are based on the works by [Shahabsafa et al. \(2018\)](#) for the discrete TSO problem.

Define  $\mathcal{S}$  as the set of candidate nonzero cross-sectional areas of bars:

$$\mathcal{S} = \{s_1, s_2, \dots, s_v\},$$

where  $0 < s_1 < s_2 < \dots < s_v$  and  $v$  is the cardinality of set  $\mathcal{S}$ . Without loss of generality, we may assume that the number of candidate sizes is the same for all the bars. Furthermore, for ease of presentation, we assume that all the bars have the same set  $\mathcal{S}$  of potential cross-sectional areas. We use  $\mathcal{K} = \{1, \dots, v\}$  to denote the set of indices corresponding to the discrete set  $\mathcal{S}$ . The cross-sectional area of bar  $i$ , for  $i \in \mathcal{I}$ , takes values from the set  $\{0\} \cup \mathcal{S}$  in the discrete TTDSO problem. We define binary decision variable  $y_i$ , for  $i \in \mathcal{I}$ , as

$$y_i = \begin{cases} 1, & \text{if } x_i > 0, \\ 0, & \text{otherwise.} \end{cases} \quad (6)$$

If  $y_i = 1$ , then bar  $i$  gets a nonzero cross-sectional area, and if  $y_i = 0$ , then bar  $i$  has a zero cross-sectional area and disappears from the structure. Let  $\sigma_{ik}$ , for  $i \in \mathcal{I}$  and  $k \in \mathcal{K}$ , be defined as

$$\sigma_{ik} = \begin{cases} \lambda_i \Delta l_i, & \text{if } x_i = s_k, \\ 0, & \text{otherwise.} \end{cases} \quad (7)$$

Variable  $\sigma_{ik}$  represents the stress on bar  $i$  if its cross-sectional area is equal to  $s_k$ ; otherwise,  $\sigma_{ik}$  is zero. Thus we have that

$$\sigma_i = \sum_{k \in \mathcal{K}} \sigma_{ik}.$$

Additionally, we define  $\sigma_i^d$  as

$$\sigma_i^d = \begin{cases} \lambda_i \Delta l_i, & \text{if } x_i = 0, \\ 0, & \text{otherwise.} \end{cases} \quad (8)$$

Variable  $\sigma_i^d$ , for  $i \in \mathcal{I}$ , is a dummy variable and is equal to zero if bar  $i$  takes a nonzero cross-sectional area. However, if  $x_i = 0$ , then  $\sigma_i^d$  takes a nonzero value. Then, from equations (7) and (8), we have that

$$\lambda_i \Delta l_i = \sum_{k \in \mathcal{K}} \sigma_{ik} + \sigma_i^d. \quad (9)$$

[Sved and Ginos \(1968\)](#) demonstrated that when a bar has a zero cross-sectional area, the Euler buckling and yield stress constraints must become inactive for that bar. As in equation (9), all variables  $\sigma_{ik}$ , for  $k \in \mathcal{K}$ , can be equal to zero by introducing variable  $\sigma_i^d$ . Thus, introducing dummy stress variables ensures that the Euler buckling and yield stress constraints become inactive if the cross-sectional area of a bar is zero.

To enforce that  $x_i \in \{0\} \cup \mathcal{S}$ , for all  $i \in \mathcal{I}$ , we use the *incremental model* proposed by [Shahabsafa et al. \(2018, Section 2.2\)](#). Let  $\bar{\mathcal{K}} = \{1, \dots, v-1\}$  and  $\delta_k = s_{k+1} - s_k$  for  $k \in \bar{\mathcal{K}}$ . In the incremental model of the discrete TTDSO problem, the cross-sectional areas of the bars are given as:

$$\begin{aligned} x_i &= s_1 y_i + \sum_{k \in \bar{\mathcal{K}}} \delta_k z_{ik}, & i \in \mathcal{I}, \\ y_i &\geq z_{i1}, & i \in \mathcal{I}, \\ z_{i,k-1} &\geq z_{ik}, & i \in \mathcal{I}, k \in \bar{\mathcal{K}} \setminus \{1\}, \\ y_i &\in \{0, 1\}, & i \in \mathcal{I}, \\ z_{ik} &\in \{0, 1\}, & i \in \mathcal{I}, k \in \bar{\mathcal{K}}. \end{aligned} \quad (10)$$

If  $y_i = 1$  and  $z_{i1} = 0$ , then  $x_i = s_1$ . If  $z_{i,k-1} = 1$  and  $z_{ik} = 0$ , then  $x_i = s_k$ . If  $z_{i,v-1} = 1$ , then  $x_i = s_v$ .

The following set of constraints are needed to enforce yield stress and Euler buckling constraints

$$\begin{aligned}
& \max(-\gamma_i s_1, \sigma_i^{\min}) (y_i - z_{i1}) \leq \sigma_{i1} \leq \sigma_i^{\max} (y_i - z_{i1}), & i \in \mathcal{I}, \\
& \max(-\gamma_i s_k, \sigma_i^{\min}) (z_{i,k-1} - z_{ik}) \leq \sigma_{ik} \leq \sigma_i^{\max} (z_{i,k-1} - z_{ik}), & i \in \mathcal{I}, k \in \bar{\mathcal{K}} \setminus \{1\}, \\
& \max(-\gamma_i s_v, \sigma_i^{\min}) z_{i,v-1} \leq \sigma_{iv} \leq \sigma_i^{\max} z_{i,v-1}, & i \in \mathcal{I}, \\
& (1 - y_i) \underline{\sigma}_i^d \leq \sigma_i^d \leq (1 - y_i) \bar{\sigma}_i^d, & i \in \mathcal{I}.
\end{aligned} \tag{11}$$

From constraints (11), it follows that if  $y_i = 0$ , then  $\sigma_{ik} = 0$ , for all  $k \in \mathcal{K}$ , and  $\underline{\sigma}_i^d \leq \sigma_i^d \leq \bar{\sigma}_i^d$ , where

$$\begin{aligned}
\underline{\sigma}_i^d &= \lambda_i \left( \sum_{\ell | r_{i\ell} < 0} r_{i\ell} u_\ell^{\max} + \sum_{\ell | r_{i\ell} > 0} r_{i\ell} u_\ell^{\min} \right), \\
\bar{\sigma}_i^d &= \lambda_i \left( \sum_{\ell | r_{i\ell} < 0} r_{i\ell} u_\ell^{\min} + \sum_{\ell | r_{i\ell} > 0} r_{i\ell} u_\ell^{\max} \right).
\end{aligned} \tag{12}$$

Equations (12) are obtained from (3), (4), and (5). If  $y_i = 1$ , which implies that  $x_i > 0$ , then  $\sigma_i^d = 0$ . In addition, if  $z_{i,\bar{k}-1} = 1$  and  $z_{i\bar{k}} = 0$ , then  $\sigma_{ik} = 0$ , for all  $k \neq \bar{k}$  and  $\max(-\gamma_i s_{\bar{k}}, \sigma_i^{\min}) \leq \sigma_{i\bar{k}} \leq \sigma_i^{\max}$ .

The incremental model for the TTDSO problem is as follows:

$$\begin{aligned}
\min & \sum_{i \in \mathcal{I}} \rho_i x_i, \\
\text{s.t.} & Rq = f, \\
& R^T u = \Delta l, \\
& x_i - s_1 y_i - \sum_{k \in \bar{\mathcal{K}}} \delta_k z_{ik} = 0, & i \in \mathcal{I}, \\
& \lambda_i \Delta l_i - \sum_{k \in \mathcal{K}} \sigma_{ik} - \sigma_i^d = 0, & i \in \mathcal{I}, \\
& q_i - \sum_{k \in \mathcal{K}} s_k \sigma_{ik} = 0, & i \in \mathcal{I}, \\
& \max(-\gamma_i s_1, \sigma_i^{\min}) (y_i - z_{i1}) \leq \sigma_{i1} \leq \sigma_i^{\max} (y_i - z_{i1}), & i \in \mathcal{I}, \\
& \max(-\gamma_i s_k, \sigma_i^{\min}) (z_{i,k-1} - z_{ik}) \leq \sigma_{ik} \leq \sigma_i^{\max} (z_{i,k-1} - z_{ik}), & i \in \mathcal{I}, k \in \bar{\mathcal{K}} \setminus \{1\}, \\
& \max(-\gamma_i s_v, \sigma_i^{\min}) z_{i,v-1} \leq \sigma_{iv} \leq \sigma_i^{\max} z_{i,v-1}, & i \in \mathcal{I}, \\
& (1 - y_i) \underline{\sigma}_i^d \leq \sigma_i^d \leq (1 - y_i) \bar{\sigma}_i^d, & i \in \mathcal{I}, \\
& u_\ell^{\min} \leq u_\ell \leq u_\ell^{\max}, & \ell \in \mathcal{L}, \\
& z_{i1} \leq y_i, & i \in \mathcal{I}, \\
& z_{ik} \leq z_{i,k-1}, & i \in \mathcal{I}, k \in \bar{\mathcal{K}} \setminus \{1\}, \\
& y_i \in \{0, 1\}, & i \in \mathcal{I}, \\
& z_{ik} \in \{0, 1\}, & i \in \mathcal{I}, k \in \bar{\mathcal{K}}.
\end{aligned} \tag{13}$$

An alternative to model (13) for the discrete TTDSO problem can be obtained by considering, instead of sequential binary variables (10), a basic choice of binary variables (as in Shahabsafa et al. (2018)). The model is presented in Appendix 6.

Let  $\mathcal{N}_\ell$ , for  $\ell \in \mathcal{L}$ , be the set of the bars of the ground structure that are connected to the node corresponding to the  $\ell$ -th coordinate of the displacement vector. The following constraints enforce that if no bar is connected to a node, then the displacement of that node is zero.

$$u_\ell^{\min} \sum_{i \in \mathcal{N}_\ell} y_i \leq u_\ell \leq u_\ell^{\max} \sum_{i \in \mathcal{N}_\ell} y_i, \quad \ell \in \mathcal{L}. \tag{14}$$

Adding constraints (14) to (13) increases the solution time of the problem, but if not added, the displacements of the nodes with no bars connected to them may be nonzero. However, the optimal cross-sectional areas of the problem do not change, i.e., the optimal structure still satisfies all the constraints of the problem even if constraints (14) are not added. Thus, in what follows, instead of adding constraints (14) to the model, as a post-processing step, we set the displacements of the nodes with no bars connected to them to zero. Model (13) can be extended, as done by Mela (2014), to account for multi-scenario discrete TTDSO problems.

Model (13) differs from the model proposed by Mela (2014) in three aspects: first, the model proposed by Mela (2014) introduces a binary variable for each possible cross-sectional area of a bar, but in model (13) binary variables represent the increments in the cross-sectional areas of the bars. Second, in contrast to the model proposed by Mela (2014), we do not need to introduce binary variables for the nodes of the truss structure in model (13). Third, variables  $\sigma_i^d$ , for  $i \in \mathcal{I}$ , are introduced to ensure that yield stress and Euler buckling constraints are not enforced when a bar vanishes from the structure. In Section 5, we demonstrate that model (13) is solved significantly faster than the model proposed by Mela (2014).

## 4 Structure stability

In this section, we first propose necessary conditions for the kinematic stability of a truss structure. Then, we propose a method to avoid kinematically unstable structures. While our method is new, it is similar in a spirit to the methods proposed by Faustino et al. (2006) and Mela (2014). Most importantly, we prove that, with probability one, the truss structures obtained by our method are kinematically stable. In what follows, we refer to the truss corresponding to cross-sectional areas given by  $x \in \mathbb{R}^m$  as *structure*  $x$ . We need the following definitions to present the results.

**Definition 4.1** (Active bars). *Active bars of structure  $x$  are the bars whose cross-sectional area is greater than zero. The index set of the active bars of structure  $x$  is denoted by  $\mathcal{I}^x$ .*

**Definition 4.2** (Active nodes). *An active node in structure  $x$  is a pinned node, which is connected to at least one active bar. The index set of active nodes of structure  $x$  is denoted by  $\mathcal{J}^x$ .*

**Definition 4.3** (Active coordinates). *The set of active coordinates in structure  $x$  is the set of the coordinates corresponding to active nodes in structure  $x$ . The index set of the active coordinates is denoted by  $\mathcal{L}^x$ .*

In what follows, vectors and matrices are defined in the reduced space of the active nodes and active bars. Let  $m^x$  and  $n^x$  denote the number of active bars and the degrees of freedom of active nodes of structure  $x$ , respectively, i.e.,  $m^x = |\mathcal{I}^x|$  and  $n^x = |\mathcal{J}^x| \times d$ .

**Definition 4.4** (Reduced topology matrix). *The reduced topology matrix of structure  $x$ , denoted by  $R^x \in \mathbb{R}^{n^x \times m^x}$ , is the topology matrix corresponding to active nodes and active bars.*

**Definition 4.5** (Reduced stiffness matrix). *The reduced stiffness matrix of structure  $x$ , denoted by  $K^x(x) \in \mathbb{R}^{n^x \times n^x}$ , is the stiffness matrix corresponding to the set of active nodes  $\mathcal{J}^x$ :*

$$K^x(x) = \sum_{i \in \mathcal{I}^x} x_i \lambda_i r_i^x (r_i^x)^T, \quad (15)$$

where  $r_i^x \in \mathbb{R}^{n^x}$  is the topology vector corresponding to the  $i$ -th bar (i.e.  $i$ -th column of topology matrix  $R^x$ ) in the lower dimensional space of the active nodes of structure  $x$ .

The reduced nodal displacements and reduced external force vector of structure  $x$ , respectively denoted by  $u^x$  and  $f^x$ , are the vectors of the nodal displacements and external forces in the lower-dimensional space of the active nodes.

**Definition 4.6** (Kinematic stability). *A truss structure with cross-sectional area  $x \in \mathbb{R}^m$  is kinematically stable if  $(R^x)^T u^x = 0$  implies  $u^x = 0$  (Hajela and Lin, 1992; Rajasekaran and Sankarasubramanian, 2001).*

**Remark 4.7.** Given that matrix  $K^x(x)$  is positive semi-definite, the stability condition of Definition 4.6 is equivalent to each of the following conditions:

- $\text{rank}(R^x) = n^x$
- $\det(K^x(x)) > 0$ ; hence,  $K^x(x)$  is positive definite.

If structure  $x$  is not stable, then it is called an unstable structure.

## 4.1 Necessary conditions for truss kinematic stability

We propose necessary conditions for the stability of a truss structure and derive a set of constraints based on those necessary conditions that are used to strengthen formulation (13) to reduce the solution time of discrete TTDSO problems. To derive the necessary conditions, we need the following definition:

**Definition 4.8** (Orientation vector). *The orientation vector of a bar with respect to one of its end nodes is the unit vector, which starts from that node pointing to the other node in the direction of the bar.*

Suppose the coordinate system is specified. The coordinates of the topology vector  $r_i$ , for  $i \in \mathcal{I}$ , corresponding to one of the end nodes of bar  $i$  are equal to the negative of the orientation vector of bar  $i$  with respect to that end node. The coordinates of the topology vector corresponding to the nodes that are not connected to bar  $i$  are zero.

**Proposition 4.9.** *If a truss structure is stable, for any active node, the orientation vectors connected to that node span the space  $\mathbb{R}^d$ .*

*Proof.* Suppose that we have a stable structure  $x$ . We prove the result by contradiction. We assume that there exists an active node in the structure whose set of orientation vectors, corresponding to the active bars connected to that node, do not span the space  $\mathbb{R}^d$ .

Let  $\bar{R} \in \mathbb{R}^{d \times m^x}$  be the sub-matrix formed by taking the rows of matrix  $R^x$  corresponding to the degrees of freedom of that node. The nonzero columns of matrix  $\bar{R}$  are multiples of the respective orientation vectors of the active bars connected to that node. Since the set of the orientation vectors do not span the space, we have  $\text{rank}(\bar{R}) < d$ , which implies that matrix  $R^x$  is not full row rank. Hence, we conclude that  $\text{rank}(R^x) < n^x$ . This contradicts the stability condition, as noted in Remark 4.7.  $\square$   $\square$

**Remark 4.10.** *In a two-dimensional space, an active node in a stable structure has to be connected to at least two bars that are not on one line.*

**Remark 4.11.** *In a three-dimensional space, an active node in a stable structure has to be connected to at least three bars that are not in one plane.*

Let the sets  $\mathcal{B}_j$  and  $\mathcal{B}_j^x$ , for  $j \in \mathcal{J}$ , be the set of bar indices connected to node  $j$  in the ground structure and in structure  $x$ , respectively. From Proposition 4.9, we know that the number of active bars connected to a node should be more than or equal to the dimension of the space. The following constraints ensure this necessary condition:

$$y_i d \leq \sum_{h \in \mathcal{B}_j} y_h, \quad i \in \mathcal{B}_j, j \in \mathcal{J}. \quad (16)$$

Let set  $\mathcal{Q}_j$  contain the sets  $\bar{\mathcal{Q}}_j$  of bar indices of the ground structure that are connected to node  $j$  such that  $|\bar{\mathcal{Q}}_j| \geq d$  and the orientation vectors of the respective bars do not span the space  $\mathbb{R}^d$ . In other words, if  $\mathcal{B}_j^x = \bar{\mathcal{Q}}_j$ , for node  $j \in \mathcal{J}^x$ , and for  $\bar{\mathcal{Q}}_j \in \mathcal{Q}_j$ , then structure  $x$  is not stable.

From Proposition 4.9, we know that, for all  $\bar{\mathcal{Q}}_j \in \mathcal{Q}_j$ , if  $\sum_{i \in \bar{\mathcal{Q}}_j} y_i = |\bar{\mathcal{Q}}_j|$ , then we must have  $\sum_{i \in \mathcal{B}_j \setminus \bar{\mathcal{Q}}_j} y_i \geq 1$ . This condition is enforced by adding the following constraints:

$$\sum_{i \in \bar{\mathcal{Q}}_j} y_i \leq |\bar{\mathcal{Q}}_j| - 1 + \sum_{i \in \mathcal{B}_j \setminus \bar{\mathcal{Q}}_j} y_i, \quad \bar{\mathcal{Q}}_j \in \mathcal{Q}_j, j \in \mathcal{J}. \quad (17)$$

Figure 1 shows a simple instance in a three-dimensional space where five bars are connected to node  $j$ . In that case, set  $Q_j$  is defined as:

$$Q_j = \{\{1, 2, 3\}, \{1, 2, 4\}, \{1, 3, 4\}, \{2, 3, 4\}, \{1, 2, 3, 4\}\},$$

where none of the sets included in  $Q_j$  span the three-dimensional space.

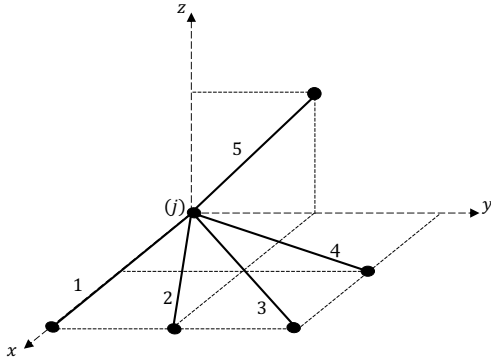


Figure 1: A simple instance of bars connected to a given node  $j$  with  $d = 3$ .

## 4.2 Enforcing kinematic stability by external force perturbation

In this section, we propose a method that enforces all the solutions of the discrete TTDSO problem to be kinematically stable structures. The method is similar to the ones proposed by [Faustino et al. \(2006\)](#) and by [Mela \(2014\)](#) in that it is based on perturbing the external forces of the truss. [Faustino et al. \(2006\)](#) developed an optimization model based on a perturbation of the external forces and provided the intuition of why their proposed perturbation results in a stable structure. However, they did not specify the characteristics of their proposed random perturbation, which are necessary to ensure kinematically stable trusses. [Mela \(2014\)](#) employed a predefined perturbation, which resembles the perturbation proposed by [Faustino et al. \(2006\)](#). Empirically, [Mela \(2014\)](#) observed that for all the considered discrete TTDSO problem instances, solving the perturbation model gave a kinematically stable structure. Neither [Faustino et al. \(2006\)](#) nor [Mela \(2014\)](#) proved that their proposed perturbation methodology is guaranteed to eliminate unstable structures. Here, we modify the perturbation methodology that proposed by the two articles cited above and rigorously prove that the truss structures obtained by our perturbation method are kinematically stable.

Let  $\mathcal{N}_\ell^x$ , for  $\ell \in \mathcal{L}$ , be the set of the bars of structure  $x$  with nonzero cross-sectional area that are connected to the node corresponding to the  $\ell$ -th coordinate of the external force. We assume that the perturbation vector of the external forces, denoted by  $p \in \mathbb{R}^n$ , is randomly generated as follows:

$$p_\ell = \sum_{i \in \mathcal{N}_\ell} p_{\ell i} y_i, \quad \ell \in \mathcal{L}, \quad (18)$$

where  $p_{\ell i}$ , for  $\ell \in \mathcal{L}, i \in \mathcal{I}$ , are independent random variables with normal distribution with mean zero and variance  $\epsilon^2$  where  $\epsilon$  is a small positive real number. If  $\epsilon$  is a large number, then the perturbation of the external forces may potentially change the optimal solution of the problem. On the other hand, if  $\epsilon$  is too small, it may lead to numerical instability when solving the problem. Notice that as defined by equation (18), the random vector  $p$  is a function of the decision variable  $y \in \mathbb{R}^m$ . Let  $p^x$ , for structure  $x \in \mathbb{R}^m$ , be the reduced perturbation vector in the lower dimensional space of the active nodes.

**Proposition 4.12.** *The reduced vector  $p^x$ , for a given  $x \in \mathbb{R}^m$ , has an  $n^x$ -variate normal distribution.*

*Proof.* Let  $x \in \mathbb{R}^m$  be given. From the set of constraints (6), we know that  $y_i = 0$ , for  $i \in \mathcal{I}$ , if  $x_i = 0$ . So we rewrite the perturbation vector  $p$  for the given  $x$  as

$$p_\ell = \begin{cases} \sum_{i \in \mathcal{N}_\ell^x} p_{\ell i} & \text{if } \ell \in \mathcal{L}^x, \\ 0 & \text{otherwise,} \end{cases} \quad \ell \in \mathcal{L}. \quad (19)$$

We know that  $|\mathcal{L}^x| = n^x$ ; thus, the perturbation vector  $p$  for given  $x$  has  $n^x$  nonzero coordinates, each of which is a sum of independent normally distributed random variables. Thus, for  $\ell \in \mathcal{L}^x$ ,  $p_\ell$  has a normal distribution with mean zero and variance  $|\mathcal{N}_\ell^x| \epsilon^2$ . Additionally, the coordinates of the vector  $p^x$  are independent from each other. Thus, vector  $p^x$  has a multivariate normal distribution.  $\square$   $\square$

The perturbed external force  $\bar{f} \in \mathbb{R}^n$  is defined as:

$$\bar{f} = f + p. \quad (20)$$

We prove that if the perturbed external force  $\bar{f}$  is considered, with probability one, any feasible solution of the incremental model (13) is stable. Let  $\bar{f}^x$ , for structure  $x \in \mathbb{R}^m$ , be the reduced vector of the perturbed external force  $\bar{f}$  in the lower-dimensional space of the active nodes.

**Lemma 4.13.** *Let structure  $x \in \mathbb{R}^m$  be unstable. Then the probability that the system of equations  $K^x(x)u^x = \bar{f}^x$  has a solution for  $u^x \in \mathbb{R}^{n^x}$  is zero.*

*Proof.* Let  $x \in \mathbb{R}^m$  be given. Next, we compute the probability that the following equations hold for structure  $x$ :

$$K^x(x)u^x = \bar{f}^x = f^x + p^x. \quad (21)$$

From this equation, we have  $f^x + p^x \in \text{col}(K^x(x))$ , where  $\text{col}(K^x(x))$  is the column space of matrix  $K^x(x)$ . Thus,  $p^x \in \text{col}(K^x(x)) - \{f^x\}$ .

Since structure  $x$  is kinematically unstable, from Definition 4.6, it follows that  $\det(K^x(x)) = 0$ . Therefore,  $\dim(\text{col}(K^x(x))) < n^x$ , and thus,

$$\dim(\text{col}(K^x(x)) - \{f\}) < n^x.$$

From Proposition 4.12, the random vector  $p^x$  has an  $n^x$ -variate normal distribution. Therefore, we conclude that the probability that  $p^x \in \text{col}(K^x(x)) - \{f^x\}$ , i.e., that  $p^x$  is in a subspace with dimension less than  $n^x$ , is zero. Thus, the probability that the set of equations (21) holds for an unstable structure is zero.  $\square$   $\square$

**Corollary 4.14.** *The probability that an unstable structure  $x \in \mathbb{R}^m$  is feasible for problem (13) with perturbed external force  $\bar{f}$  is zero.*

*Proof.* Let  $x \in \mathbb{R}^m$  be given. If  $K(x)u = \bar{f}$  holds then  $K^x(x)u^x = \bar{f}^x$  is satisfied for structure  $x$ . Thus, from Lemma 4.13, we conclude that equations  $K(x)u = f$  hold for unstable structure  $x$  with probability zero. Additionally, we know that the equation system  $K(x)u = f$  is equivalent to the following set of constraints Shahabsafa et al. (2018):

$$\begin{aligned} Rq &= f, \\ R^T u &= \Delta l, \\ \lambda \Delta l &= \sigma, \\ q_i &= x_i \sigma_i, \quad i \in \mathcal{I}. \end{aligned}$$

Thus, the probability that an unstable solution  $x$  is feasible is zero.  $\square$   $\square$

**Theorem 4.15.** *The probability that the feasible set of problem (13) with perturbed external force  $\bar{f}$ , as defined in (20), includes a kinematically unstable structure is zero.*

*Proof.* In the discrete TTDSO problem (13), cross-sectional area  $x_i$ , for  $i \in \mathcal{I}$ , takes values from discrete set  $\mathcal{S} \cup \{0\}$ . So the set of possible structures in problem (13) is finite, and thus, the set of possible unstable structures is finite. Suppose set  $\mathcal{X} = \{x^1, x^2, \dots, x^\tau\}$  is the set of unstable structures that are feasible for problem (13), where  $x^k \in \mathbb{R}^m$  for  $k = 1, \dots, \tau$  are the cross-sectional area vectors corresponding to each of the unstable problem solutions. Let  $\mathcal{E}_k$ , for  $k = 1, \dots, \tau$ , denote the event that structure  $x^k$  is infeasible for problem (13) with perturbed external force  $\bar{f}$ , and let  $\mathcal{F}_k$  be the complement of  $\mathcal{E}_k$ , that is,  $\mathcal{F}_k$  is the event that structure  $x^k$  is feasible for the perturbed version of problem (13). Next, we calculate the probability of the event that all the structures from set  $\mathcal{X}$  are infeasible. That is, we compute  $\Pr(\bigcap_{k=1}^{\tau} \mathcal{E}_k)$ . Notice that

$$\bigcap_{k=1}^{\tau} \mathcal{E}_k = \left( \bigcup_{k=1}^{\tau} \mathcal{E}_k^c \right)^c = \left( \bigcup_{k=1}^{\tau} \mathcal{F}_k \right)^c.$$

From Lemma 4.13, it follows that  $\Pr(\mathcal{F}_k) = 0$  for  $k = 1, \dots, \tau$ . Thus,  $\Pr(\bigcup_{k=1}^{\tau} \mathcal{F}_k) = 0$ , or equivalently

$$\Pr\left(\bigcap_{k=1}^{\tau} \mathcal{E}_k\right) = 1.$$

Therefore, the probability that all the unstable structures are infeasible is one, i.e., the probability that the feasible set of the problem with perturbation (20) includes a kinematically unstable structure is zero.  $\square$   $\square$

## 5 Numerical results

In this section, we present our numerical results. First, we compare model (13) with and without random perturbation of the external forces to demonstrate the impact of the perturbation on the stability of the structure obtained from model (13). Moreover, we demonstrate the impact of adding necessary constraints (16) and (17) on the solution time of model (13). Finally, we compare the solution time and weight of the solution obtained from model (13) with those of the model proposed by Mela (2014).

The numerical results are run on a machine with Dual Intel Xeon® CPU 4114 @ 2.20 GHz (20 cores) and 128 GB of RAM. GuRoBi 8.1.1 (2019) is used to solve the MILO models, which has the capability of using multiple threads in solving a MILO problem with the branch and bound algorithm and is set to use 10 threads in solving the MILO models. Since GuRoBi exhausts memory in solving the MILO models, the `NodefileStart` parameter is set to 64 GB, which limits the memory to that amount. When the memory is at the limit, the nodes are compressed and written to a local disk. The maximum solution time is set to one day. Other GuRoBi parameters remain at the default values.

### 5.1 Michell Structure

Michell trusses (Sokół, 2011), which are widely used scalable two-dimensional truss problems, are used to obtain the numerical results. A Michell truss is defined by four parameters:  $n_\xi, n_\eta, d_\xi, d_\eta$ . The first two stand for the number of blocks in the  $\xi$  and  $\eta$  directions and the last two describe the connectivity of diagonal bars in the ground structure, respectively. The Michell truss has  $(n_\xi + 1) \times (n_\eta + 1)$  nodes. Node  $(i, j)$ , for  $0 \leq i \leq n_\xi$  and  $0 \leq j \leq n_\eta$ , is connected to node  $(i', j')$  in the ground structure, if  $i - d_\xi \leq i' \leq i + d_\xi$  and  $j - d_\eta \leq j' \leq j + d_\eta$  and there is no overlapping bar in the middle. If two bars overlap, we eliminate the longest bar from the ground structure (Sokół, 2011). If overlapping bars are allowed in the ground structure, then chain eliminating constraints must be added (Mela, 2014). In a Michell truss, bars can cross each other, but one can add constraints to the model to avoid crossing bars in a feasible structure. Nodes  $(0, n_\eta/4)$  and  $(0, 3n_\eta/4)$  are fixed. A downward external force  $f_0$  is exerted on node  $(n_\xi, n_\eta/2)$ . In Figure 2, Michell ground structure 8-4-2-2 with its associated external force is demonstrated.

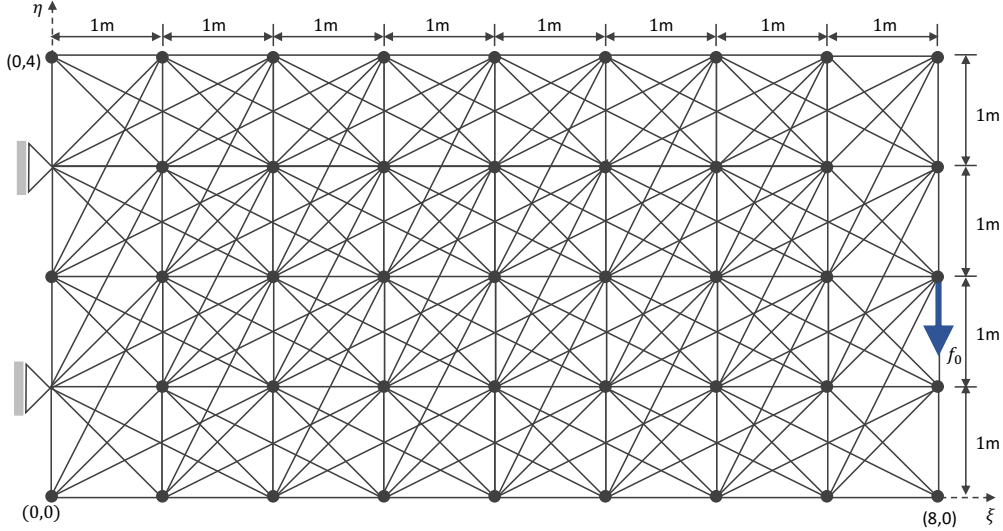


Figure 2: Michell truss ground structure 8-4-2-2.

The discrete set of candidate radii of the cross-sectional areas of the bars in the Michell truss is  $\{2, 2.5, 3, \dots, 8\}$  cm, and  $\pi = 3.14$ . In Table 1, parameters of the Michell trusses are given. The data of the Michell trusses that are solved in this study are made publicly available<sup>1</sup>.

Table 1: Parameters used in Michell trusses.

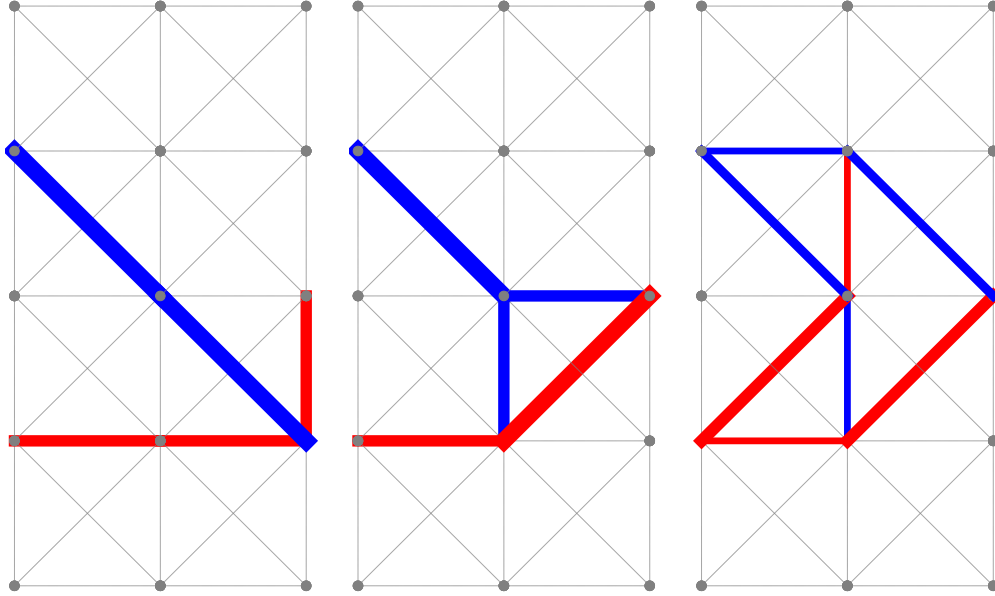
Property	Value
$f_0$	$8 \times 10^5$ N
$\epsilon$	$4.61 \times 10^2$ N
$\rho$	$27.68$ kg/m <sup>3</sup>
$E$	69 GPa
$u^{\max}$	$2n_\xi$ cm
$u^{\min}$	$-2n_\xi$ cm
$\sigma^{\max}$	172.36 MPa
$\sigma^{\min}$	-172.36 MPa

## 5.2 Impact of external force perturbation and necessary conditions

In this section, we examine the impact of adding constraints (16) and (17) and the external force perturbation (18) to model (13).

The optimal structure of the Michell truss 2-4-1-1 is shown in Figure 3. Figure 3a is the optimal structure obtained by solving model (13) without constraints (16) and (17) and without the external force perturbation. The solution is not stable. Figure 3b is the optimal structure obtained by solving model (13) with constraints (16) and (17). The structure is still unstable, which demonstrates that constraints (16) and (17) are not sufficient to obtain a kinematically stable structure. However, the structure shown in Figure 3c, which is obtained by adding the external force perturbation to model (13) is stable. The reduced stiffness matrices of the structures in Figure 3a and 3b are singular, while the reduced stiffness matrix of structure in Figures 3c is positive definite and thus non-singular.

<sup>1</sup><https://github.com/shahabsafa/truss-data.git>



a) Without constraints (16) and (17) and without perturbation (20). The structure is **unstable**.  
b) With constraints (16) and (17), but without perturbation (20). The structure is **unstable**.  
c) Without constraints (16) and (17), but with perturbation (20). The structure is **stable**.

Figure 3: Impact of adding constraints (16) and (17) and external force perturbation to model (13) on the kinematic stability of Michell truss 2-4-1-1.

We now compare the solution time and the weight of the structures obtained from model (13) with and without external force perturbation. Additionally, we analyze the impact of adding constraints (16) and (17) on the solution time and weights of the structures obtained from model (13) with the external force perturbation. As shown in Table 2, the solutions of model (13) without adding an external force perturbation are not stable, which demonstrates the need for adding a perturbation to ensure structure stability. Moreover, adding constraints (16) and (17) to model (13) with the external force perturbation helps to significantly reduce the solution time for many of the Michell truss instances.

Figure 4 shows the Michell truss 7-4-1-1 obtained by solving model (13) with constraints (16) and (17) and external force perturbation (20) with 24 hours solution time budget. The blue bars are under tension while the red bars are under compression. We show the distribution of yield stress and Euler buckling stress in Figures 4a and 4b, respectively. If we ignore Euler buckling constraints, the structure would become symmetric. However, because of the Euler buckling constraints and discrete cross sectional areas, the optimal structure is not necessarily symmetric.

### 5.3 Comparison of the incremental model with the Mela's model

In this section, we compare model (13), with constraints (16) and (17) added, with the model proposed by Mela (2014). In both models perturbations of the external forces are considered, though perturbation in the two models are different. In Table 3,  $t$  and  $w$  denote the solution time and the weight of the structure obtained from the model proposed by Mela (2014), respectively; and  $t'$  and  $w'$  denote the solution time and the weight of the structure obtained from model (13), respectively.

Table 2: Weights (kg) and solution times (s) for the proposed model with and without external force perturbation (20) and constraints (16) and (17).

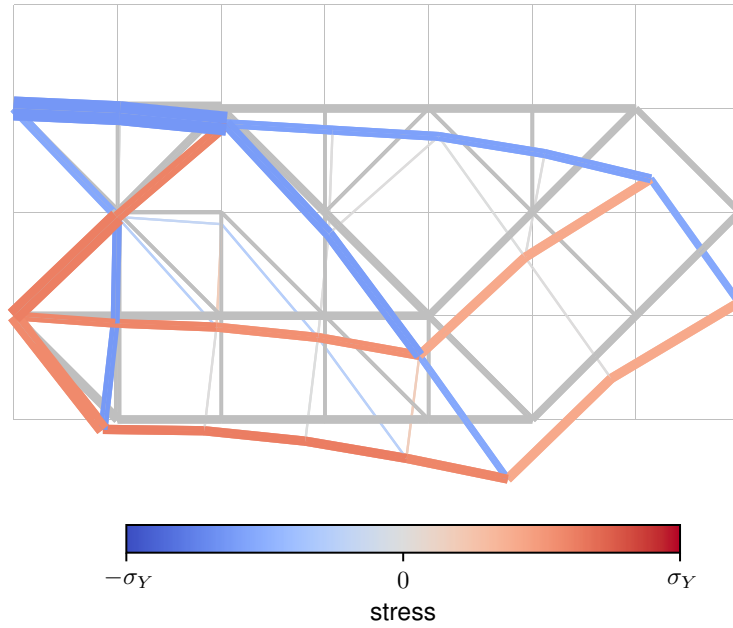
Problem ( $n_\xi$ - $n_\eta$ - $d_\xi$ - $d_\eta$ )	w/o perturbation (20) and w/o condrs. (16, 17)			w/ perturbation (20) and w/o condrs. (16, 17)		w/ perturbation (20) and w/ condrs. (16, 17)	
	sol. time	weight	stable	sol. time	weight	sol. time	weight
1-4-1-1	0.04	33.87	1	0.11	33.87	0.09	33.87
2-4-1-1	2.49	98.26	1	2.26	98.26	2.35	98.26
3-4-1-1	3.61	154.86	0	13.17	162.65	7.91	162.65
4-4-1-1	165.35	239.01	0	48862.00	253.07	8574.00	253.07
5-4-1-1	1062.44	326.20	0	86400.00	339.76	28389.00	339.76
6-4-1-1	86400.00	433.34	0	86400.00	461.04	86400.00	457.32
7-4-1-1	86400.00	552.35	0	86400.00	584.60	86400.00	585.22
8-4-1-1	86400.00	662.81	0	86400.00	724.32	86400.00	719.77
2-4-2-2	0.88	84.29	1	0.88	84.29	0.91	84.29
3-4-2-2	8.68	149.30	0	103.65	157.50	31.36	157.50
4-4-2-2	129.42	222.66	0	46992.00	235.85	6122.00	235.85
5-4-2-2	3271.16	311.10	0	86400.00	325.23	86400.00	325.23
6-4-2-2	86400.00	407.62	0	86400.00	430.87	86400.00	436.50

Table 3: Weights (kg) and the solution times (s) for proposed model and Mela (2014) model.

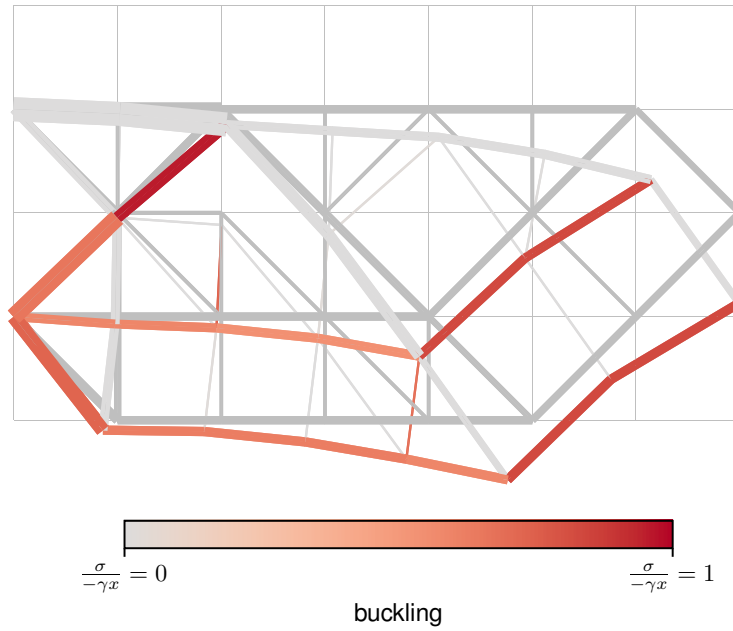
Problem ( $n_\xi$ - $n_\eta$ - $d_\xi$ - $d_\eta$ )	Mela (2014) model		Model (13)		$t/t'$	$w/w'$
	$t$	$w$	$t'$	$w'$		
1-4-1-1	0.25	33.87	0.09	33.87	3.57	1.000
2-4-1-1	7.58	98.26	2.35	98.26	3.23	1.000
3-4-1-1	453.13	162.65	7.91	162.65	57.29	1.000
4-4-1-1	86400	253.07	8574	253.07	10.07	1.000
5-4-1-1	86400	346.65	28389	339.76	3.03	1.020
6-4-1-1	86400	464.53	86400	457.32	1.00	1.016
7-4-1-1	86400	621.94	86400	585.22	1.00	1.063
8-4-1-1	86400	–	86400	719.77	1.00	$\infty$
9-4-1-1	86400	–	86400	846.60	1.00	$\infty$
2-4-2-2	1.19	84.29	0.91	84.29	1.31	1.000
3-4-2-2	282.33	157.50	31.36	157.50	9.00	1.000
4-4-2-2	86400	236.04	6122	235.85	14.11	1.000
5-4-2-2	86400	330.56	86400	325.23	1.00	1.016
6-4-2-2	86400	446.32	86400	436.50	1.00	1.022
7-4-2-2	86400	–	86400	560.02	1.00	$\infty$
8-4-2-2	86400	–	86400	683.23	1.00	$\infty$
9-4-2-2	86400	–	86400	879.08	1.00	$\infty$
6-4-3-3	86400	–	86400	447.38	1.00	$\infty$
7-4-3-3	86400	–	86400	590.47	1.00	$\infty$
8-4-3-3	86400	–	86400	691.29	1.00	$\infty$

From Table 3, the proposed model (13) is significantly faster and provides lighter feasible solutions than the model proposed by Mela (2014) (up to 57 times) in the instances that are solved to the global optimality.

As the problem size grows, the model proposed by Mela (2014) fails to provide a feasible solution in the one-day time limit, while our proposed model provides a relatively good solution in the 24-hour time limit.



a) Yield stress constraint plot, we have  $\sigma^{\max} = \sigma_Y, \sigma^{\min} = -\sigma_Y$ . A bar in blue indicates it under tension and a bar in red indicates it is under compression.



b) Buckling constraint plot. A bar under compression is shown in red and a bar in tension is masked with grey.

Figure 4: Stress and buckling of the proposed model's solution for the Michell truss 7-4-1-1. The undeformed structure is shown in gray in the background. For better visibility, the displacements are magnified.

## 6 Conclusions

In this paper, we developed a novel MILO model for the discrete TTDSO problem. We introduced necessary conditions that are required for a truss structure to be kinematically stable. Moreover, by introducing a novel way to handle an external force perturbation, we formally proved that, with probability one, the solutions of the MILO model are kinematically stable. We presented numerical results to demonstrate the efficacy of the proposed MILO model with external force perturbation in providing kinematically stable structures. Compared to the model proposed by Mela (2014), we demonstrated that our MILO model is up to 57 times faster in proving the optimality of the Michell trusses, and is significantly faster in achieving the optimal solution of discrete TTDSO problems when optimality is proved and reached, respectively. With our new model, we have obtained high quality solutions for Michell trusses with up to 388 potential bars, while we could not get even a feasible solution with the 24-hour time budget for Mela’s model for large structures. These results indicate that our methodology can be applied to other truss design problems and with other objectives.

It is worth mentioning that standard MILO solvers are used in this paper to solve the TTDSO problems. Special purpose solution methodologies (see e.g., Shahabsafa et al. (2018)) can be developed in the future to solve larger scale TTDSO problems.

## Acknowledgement

This research was supported by Air Force Office of Scientific Research Grant #FA9550-15-1-0222.

## Appendix

In the basic discrete model, the choice constraints for the TTDSO problem are defined as:

$$\begin{aligned}
 x_i &= \sum_{k \in \mathcal{K}} s_k z_{ik}, & i \in \mathcal{I}, \\
 \sum_{k \in \mathcal{K}} z_{ik} &= y_i, & i \in \mathcal{I}, k \in \mathcal{K}, \\
 y_i &\in \{0, 1\}, & i \in \mathcal{I}, \\
 z_{ik} &\in \{0, 1\}, & i \in \mathcal{I}, k \in \mathcal{K} \cup \{0\}.
 \end{aligned} \tag{22}$$

If  $y_i = 1$ , then bar  $i$  takes value from the discrete set  $\mathcal{S}$ , while  $y_i = 0$  enforces  $x_i = 0$  vanishes from the structure. In addition, to enforce equalities (7) and (8), the following set of constraints are needed:

$$\begin{aligned}
 (1 - y_i) \underline{\sigma}_i^d &\leq \sigma_i^d \leq (1 - y_i) \overline{\sigma}_i^d, & i \in \mathcal{I}, \\
 \max(-\gamma_i s_k, \sigma_i^{\min}) z_{ik} &\leq \sigma_{ik} \leq \sigma_i^{\max} z_{ik}, & i \in \mathcal{I}, k \in \mathcal{K}.
 \end{aligned} \tag{23}$$

The Euler buckling constraints are incorporated in the set of constraints (23) as well. The basic MILO model for topology design and sizing optimization is defined as

$$\begin{aligned}
 \min & \sum_{i \in \mathcal{I}} \rho l_i x_i, \\
 \text{s.t.} & Rq = f, \\
 & R^T u = \Delta l, \\
 & x_i - \sum_{k \in \mathcal{K}} s_k z_{ik} = 0, & i \in \mathcal{I}, \\
 & \lambda_i \Delta l_i - \sum_{k \in \mathcal{K}} \sigma_{ik} - \sigma_i^d = 0, & i \in \mathcal{I},
 \end{aligned}$$

$$\begin{aligned}
q_i - \sum_{k \in \mathcal{K}} s_k \sigma_{ik} &= 0, & i \in \mathcal{I}, \\
\sum_{k \in \mathcal{K}} z_{ik} &= y_i, & i \in \mathcal{I}, \\
\max \left( -\gamma_i s_k, \sigma_i^{\min} \right) z_{ik} &\leq \sigma_{ik} \leq \sigma_i^{\max} z_{ik} & i \in \mathcal{I}, k \in \mathcal{K}, \\
u_\ell^{\min} &\leq u_\ell \leq u_\ell^{\max}, & \ell \in \mathcal{L}, \\
(1 - y_i) \underline{\sigma}_i^d &\leq \sigma_i^d \leq (1 - y_i) \bar{\sigma}_i^d, & i \in \mathcal{I}, \\
y_i &\in \{0, 1\}, & i \in \mathcal{I}, \\
z_{ik} &\in \{0, 1\}, & i \in \mathcal{I}, k \in \mathcal{K}.
\end{aligned}$$

If  $y_i = 1$ , for  $i \in \mathcal{I}$ , then the problem reduces to a truss sizing optimization problem.

## References

- Aage, N., Andreassen, E., Lazarov, B. S., and Sigmund, O. (2017). Giga-voxel computational morphogenesis for structural design. *Nature*, 550(7674):84–86.
- Arora, J. and Wang, Q. (2005). Review of formulations for structural and mechanical system optimization. *Structural and Multidisciplinary Optimization*, 30(4):251–272.
- Ben-Tal, A. and Bendsøe, M. P. (1993). A new method for optimal truss topology design. *SIAM Journal on Optimization*, 3(2):322–358.
- Bendsøe, M. P., Ben-Tal, A., and Zowe, J. (1994). Optimization methods for truss geometry and topology design. *Structural Optimization*, 7(3):141–159.
- Brooks, T. R., Kenway, G. K. W., and Martins, J. R. R. A. (2018). uCRM: An aerostructural model for the study of flexible transonic aircraft wings. *AIAA Journal*. (In press).
- Chauhan, S. S. and Martins, J. R. R. A. (2018). Low-fidelity aerostructural optimization of aircraft wings with a simplified wingbox model using OpenAeroStruct. In *Proceedings of the 6th International Conference on Engineering Optimization, EngOpt 2018*, pages 418–431, Lisbon, Portugal. Springer.
- Dorn, W. S., Gomory, R. E., and Greenberg, H. J. (1964). Automatic design of optimal structures. *Journal de Mecanique*, 3:25–52.
- Faustino, A. M., Júdice, J. J., Ribeiro, I. M., and Neves, A. S. (2006). An integer programming model for truss topology optimization. *Investigação Operacional*, 26(1):11–127.
- Ghosh, A. and Mallik, A. K. (2002). *Theory of Mechanisms and Machines*. Affiliated East-West Press Private Limited.
- Gurobi Optimization Inc. (2019). Gurobi optimizer reference manual.
- Haftka, R. T. and Gürdal, Z. (2012). *Elements of Structural Optimization*. Springer Science & Business Media.
- Hajela, P. and Lin, C. Y. (1992). Genetic search strategies in multicriterion optimal design. *Structural Optimization*, 4(2):99–107.
- Jasa, J. P., Hwang, J. T., and Martins, J. R. R. A. (2018). Open-source coupled aerostructural optimization using Python. *Structural and Multidisciplinary Optimization*, 57(4):1815–1827.

- Kanno, Y. (2016). Global optimization of trusses with constraints on number of different cross-sections: a mixed-integer second-order cone programming approach. *Computational Optimization and Applications*, 63(1):203–236.
- Kanno, Y. (2018). Robust truss topology optimization via semidefinite programming with complementarity constraints: a difference-of-convex programming approach. *Computational Optimization and Applications*, pages 1–31.
- Kanno, Y. and Fujita, S. (2018). Alternating direction method of multipliers for truss topology optimization with limited number of nodes: A cardinality-constrained second-order cone programming approach. *Optimization and Engineering*, 19(2):327–358.
- Kanno, Y. and Guo, X. (2010). A mixed integer programming for robust truss topology optimization with stress constraints. *International Journal for Numerical Methods in Engineering*, 83(13):1675–1699.
- Kennedy, G. J. (2016). A full-space barrier method for stress-constrained discrete material design optimization. *Structural and Multidisciplinary Optimization*, 54(3):619–639.
- Mela, K. (2014). Resolving issues with member buckling in truss topology optimization using a mixed variable approach. *Structural and Multidisciplinary Optimization*, 50(6):1037–1049.
- Rajasekaran, S. and Sankarasubramanian, G. (2001). *Computational Structural Mechanics*. PHI Learning Pvt.
- Rozvany, G. I. (2009). A critical review of established methods of structural topology optimization. *Structural and multidisciplinary optimization*, 37(3):217–237.
- Shahabsafa, M., Mohammad-Nezhad, A., Terlaky, T., Zuluaga, L., He, S., Hwang, J. T., and Martins, J. R. (2018). A novel approach to discrete truss design problems using mixed integer neighborhood search. *Structural and Multidisciplinary Optimization*, 58(6):2411–2429.
- Sokół, T. (2011). A 99 line code for discretized michell truss optimization written in mathematica. *Structural and Multidisciplinary Optimization*, 43(2):181–190.
- Stolpe, M. (2004). Global optimization of minimum weight truss topology problems with stress, displacement, and local buckling constraints using branch-and-bound. *International Journal for Numerical Methods in Engineering*, 61(8):1270–1309.
- Stolpe, M. (2007). On the reformulation of topology optimization problems as linear or convex quadratic mixed 0–1 programs. *Optimization and Engineering*, 8(2):163–192.
- Stolpe, M. (2015). Truss topology optimization with discrete design variables by outer approximation. *Journal of Global Optimization*, 61(1):139–163.
- Stolpe, M. (2016). Truss optimization with discrete design variables: a critical review. *Structural and Multidisciplinary Optimization*, 53(2):349–374.
- Stolpe, M. and Svanberg, K. (2004). A stress-constrained truss-topology and material-selection problem that can be solved by linear programming. *Structural and Multidisciplinary Optimization*, 27(1):126–129.
- Sved, G. and Ginos, Z. (1968). Structural optimization under multiple loading. *International Journal of Mechanical Sciences*, 10(10):803 – 805.
- Van Mellaert, R., Lombaert, G., and Schevenels, M. (2015). Global size optimization of statically determinate trusses considering displacement, member, and joint constraints. *Journal of Structural Engineering*, 142(2):04015120.
- Zienkiewicz, O. C. and Taylor, R. L. (2005). *The Finite Element Method for Solid and Structural Mechanics*. Elsevier.